A STUDY ON PERFORMANCE OF COOLING FLOW FIELD WITH TRAPEZOID-SHAPE CHANNELS IN PEM FUEL CELL

Ebrahim Afshari, Masoud Ziaei-Rad
Department of Mechanical Engineering, Faculty of Engineering, University of Isfahan, Isfahan, Iran
Corresponding author: Masoud Ziaei-Rad, email: m.ziaeirad@eng.ui.ac.ir

REFERENCE NO

FCEL-01

Keywords:
Polymer electrolyte membrane fuel cell, Heat management, Cooling flow field, Temperature distribution uniformity, Pressure drop

ABSTRACT

In polymer electrolyte membrane fuel cells (PEMFCs) more than half of the chemical energy of hydrogen is converted into heat during the generation of electricity. This heat, If not being properly exhausted, impairs the performance and durability of cell. In this paper, parallel channels with trapezoid cross-sections are proposed for cooling flow field in PEMFC, and coolant flow and heat transfer in cooling plates are simulated numerically. The results indicate that maximum surface temperature, surface temperature difference, average surface temperature, temperature uniformity index and coolant temperature in a cell with trapezoidal cross-sections of cooling channels are lower than corresponding values in a same cell with rectangular cross-sections. Therefore, use of trapezoidal cross-sections for cooling channels can improve the cooling performance. Moreover, the pressure drop does not increase significantly in this new model. Consequently, the model is preferred to traditional configurations of flow channels in terms of thermal factors and minimum pressure drop.

1. INTRODUCTION

PEM Fuel cells that are electrochemical devices, rely on the transport of oxygen (or air) and hydrogen and product electricity, water and heat. A PEM fuel cell usually generates heat, as much as it produces electricity. Additional heat must be removed from the cell to control the temperature and keep it among a special range, since many processes such as kinetic and rate of electrochemical reactions, condensation and diffusion of water, water evaporation rate, the membrane conditions and longevity, and gas transport phenomenon in porous media, depend strongly on the cell temperature. Each of these factors affects the performance and effective lifetime of the cell [1, 2].

The temperature in PEM fuel cells should be large enough to ensure that the electrochemical reactions are doing well. Higher the temperature, larger is the rate of electrochemical reactions and consequently, the cell output power increases. On the other hand, higher temperatures can harm the membrane. Higher temperature results in the membrane drying and if the electrolyte be dried completely, the membrane ionic resistance ascends and then, the efficiency of the cell descends. When the dryness occurs locally, the electrolyte resistance increases in that region and hence, more heat is generated there, which cause more dryness of the electrolyte. This process is repeated unmanageably in order that some hot spots are created on the electrode-membrane assembly. This spots are the hard cores of burning the electrode- membrane assembly and destroying the fuel cell. On the other hand, as the temperature decreases, liquid water accumulates within the cell, which closes the pores of gas diffusion layer and avoids the oxygen to reach the catalyst layer. The liquid water can also fill in the porous media pores of the catalyst layer and reduce its effective surface. Therefore, an appropriate water management in a PEM fuel cell underlies a reasonable heat management in it. Besides, non-uniform distribution of the temperature reduces the lifetime and the reliability of the membrane. In contrast, uniform temperature distribution in the cell leads to uniform rate of electrochemical reactions in the catalyst layers. Good heat management is translated to keep the cell operating temperature among an appropriate temperature range and to make the temperature distribution uniform.

In fuel cells with more than 5kW power, a liquid (water or a dielectric fluid) is usually

used as the coolant and flows through created channels in cooling or bipolar plates [3, 4]. The flow field geometry is one of the most important factors in thermal management. Cooling flow field should be designed in such a manner that the following vital requirements are fulfilled simultaneously: (1) removing the generated heat at different working voltages, (2) minimizing the pressure drop across the flow field from the inlet to outlet, and (3) obtaining a uniform temperature distribution.

Each cooling channel design has its specific characteristics and outcomes. To attain these goals, one may use different types of cooling flow fields for water cooled PEMFC stacks. Among different types, serpentine, parallel and parallel-serpentine flow fields are the most applicable ones [4]. Parallel shape channels are the simplest ones with lowest manufacturing cost and also lower pressure drop than serpentine geometries, however their temperature distribution is more non-uniform. In order to have both of aforementioned advantages and also to improve the thermal performance of parallel model, it is very essential to investigate different geometries and dimensions of the coolant flow channels.

A number of studies on fuel cells are conducted to investigate the heat transfer issues in PEM fuel cells. Chen et al. [5] conducted a thermal analysis of the coolant flow field configuration to optimize the cooling flow field design of a PEMFC stack. They analyzed and compared six coolant flow field configurations and found that serpentine configurations have more uniform temperature distribution than the parallel configurations, but parallel-type configuration has a lower pressure drop. Adzakpa et al. [6] presented a 3D thermal model to study the temperature distribution in an air-cooling PEM fuel cell. They validated their numerical results with some experiments and showed that the temperature non-uniformity in the PEM fuel cell stack is very high (the temperatures at the top of the cell are higher than the bottom). Ravishankar and Prakash [7] proposed four different geometries for the water-cooling flow field in PEM fuel cells. They simulated numerically the flow filed and heat transfer in each configuration and compared their performance in terms of maximum surface temperature, temperature uniformity and pressure drop. Gould et al. [8] investigated the thermal performance of two flow field models numerically and compared their results with experimental data of temperature measurement obtained from an infrared thermography. They showed that infrared thermography is a useful tool for characterizing coolant flow fields in PEM fuel cells. In another work, Shimei and Wei [9] proposed a serpentine pipe of water passing through the cell for the cooling purpose. They implemented numerical modeling in their work and discussed on the effects of flow velocity, number of the pipe branches and also the pipe diameter on the temperature distribution in the cell. Afshari et al. [10] presented a novel design for the coolant fluid distributor by using a metal foam structure. In their work, the performance of the flow field with metal foam as coolant fluid distributor was simulated and compared with three other common designs. They concluded that among the studied cases, the metal foam as coolant fluid distributor is the best choice to be used as coolant flow field and has the potential of improving the thermal performance of polymer electrolyte membrane fuel cells. Yu and Jung [11] developed a thermal management strategy for PEM fuel cells with large active cell areas. The thermal management system model includes radiator, pump and fan and comparison and investigation of the trade-off between the temperature distribution effect and thepump parasitic loss.

Choi et al. [12] studied numerically the performance of cooling plates for the PEM fuel cell using 3D models. In their work, six cooling plates were designed and modified with different channel configurations; consist of typical serpentine and parallel configurations. The results include the comparison of the velocity through the channel, pressure drop, temperatures around the outlet and inlet areas of the channels, maximum surface temperature and uniformity.

Hashmi [3] investigated different flow field designs in 3D with a conjugate heat transfer condition at steady-state. Their results showed that conventional single serpentine design is better than modified single serpentine design on the basis of total entropy generation criterion, whereas the latter was found to be better on the basis of temperature uniformity. Sasmito et al. [13] evaluated numerically the placement of coolant plates with water in a PEM fuel cell stack, the coolant temperature, and coolant flow rate for four repetitive stack configurations, comprised of one cell; two cells; three cells; and four cells between each pair of coolant plates in the overall stack. Asghari et al. [4] investigated the design of cooling flow fields for a 5 kW PEM fuel cell. They employed a parallel serpentine flow field design and found that inlet/outlet manifolds of reactant gases have an influence on the temperature distribution in the bipolar plates. Lasbet et al. [14] proposed to modify the channel geometries in a PEM fuel cell to create chaotic laminar flow inside the cooling channels. The heat transfer efficiency, pressure loss and mixing properties of several chaotic 3D mini-channels were numerically evaluated and compared with conventional straight channels in their study. The results indicated that 3D chaotic channels can significantly improve the convective heat transfer performance over that of the conventional straight channels, outweighing the increase of pressure loss.

It is possible to use different shapes for the cross section of the cooling channels. Some of the geometries have been studied before for reactant gases flow channels and the gas transportation through them and also the pressure drop in fuel cell have been surveyed [15-19]. Parallel shape channels with rectangular cross-section are the common models. Looking at the previous studies on the cooling flow field design of PEM fuel cells shows that only the performance of straight parallel channels with rectangular cross section has been considered and compared with serpentine model. This means that no attempt can be found in the literatures on the optimization of a parallel channel by changing the geometry of its cross-section.

In this paper, we introduce an effective way to enhance the heat transfer and to make the temperature distribution of the cooling plates uniform. It is to implement a trapezoid flow channels design. Reviewing the literatures reveals that no research on numerical modeling of this novel design has been reported. We calculate the fluid flow and heat transfer in 15cm×15cm cooling plates of a PEM fuel cell and apply trapezoid flow channels as the coolant fluid distributor. Then, we assessed the performance of coolant flow field with trapezoid flow channels and compared it with straight flow channel of square cross-section in terms of maximum and average surface temperature, temperature uniformity and pressure drop.

2 THEORY AND CALCULATIONS

2.1 Geometric model

A PEM fuel cell consist of a membrane for ion conduction, two catalyst layer for electrochemical reaction, two gas diffusion layers (GDLs) for uniform reactant diffusion, and two bipolar plates for electron conduction and flow distribution (figure 1). The bipolar plate is used to supply reactant gases to the GDLs via flow channels that carved into the plates. Humidified hydrogen and air are supplied in the gas channels; they first diffuse through GDLs and then reach the catalyst layers. At the catalyst layer, the half-cell reaction takes place at anode and cathode sides, one is named anode where oxidation is taking place, whereas reduction is taking place at the cathode. Hydrogen atom splits into proton and electron in the anode side, which take different paths to the cathode. The proton passes through the membrane and the electrons create a separate current that can be utilized before they return to the cathode side. At the cathode, electron and proton are combined with oxygen to form water.

The gas diffusion layers serve to transport the reactant gases towards the catalyst layer through the open wet-proofed pores. In addition, they provide an interface when ionization takes place and transfer electrons

through the solid matrix. Voltage output of a single fuel cell is not enough for most practical applications. For this reason, individual fuel cells are combined to produce acceptable voltage levels. The other role of the bipolar plates is to separate different cells in a fuel cell stack. The cooling is generally achieved by liquid water that circulates through coolant flow channels formed in bipolar plates or in dedicated cooling plates [4, 20].

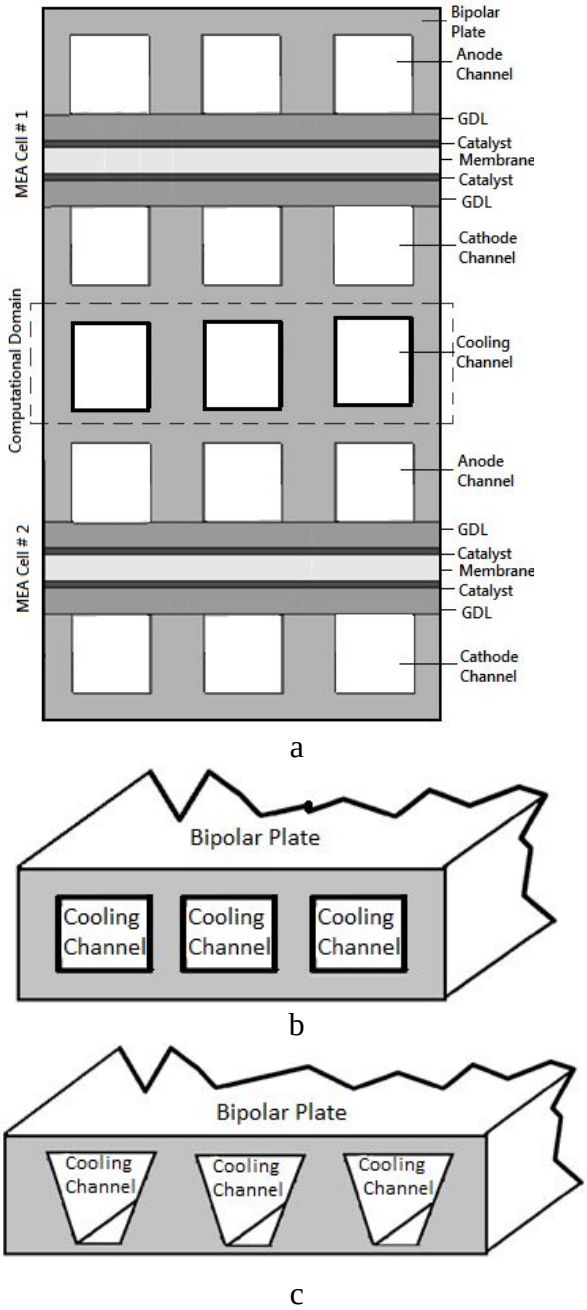

Fig. 1. a) Components of a PEM fuel cell and the modeling domain consist of a part of the cooling plate and cooling channels, b) rectangular channels c) trapezoid channels

Cooling is essential for the operation of a PEM fuel cell stack in order to exhaust the heat produced by electrochemical reactions. The computational domain in this study is a part of the cooling plate where the cooling channels are formed (figure 1). A 5kW fuel cell system is considered here for the cooling flow field design. The cooling plates have 150mm×150mm square area with machined flow channels with 37 coolant inlets.

The cooling flow field we study here consists of 37 straight parallel channels with trapezoidal cross sections. The small and large bases of the trapezoids are 1.5mm and 2mm, respectively (model A). Such cooling flow filed is propounded to improve the temperature uniformity and also to reduce the maximum surface temperature in comparison with a parallel cooling flow field with rectangular cross sections of sides 1mm and 2mm (model B). In both models, the cooling plate cross section is a 150mmx150mm square with 2mm distance between the channels and 1mm depth of channels. The cooling plate is made of graphite.

2.2 Governing equations

The Geometrical model of cooling plate and applied boundary conditions is shown in Fig. 2. The flow Reynolds number, *Re*, is set to *330* and hence, the coolant flow is laminar. Also, the flow is steady and incompressible and the coolant fluid is assumed to be Newtonian. The conservation equations of mass, momentum and energy for coolant fluid flow through the cooling plate are as follow.

$$\vec{\nabla}.\vec{u} = 0 \qquad (1)$$

$$\vec{\nabla}\cdot(\rho\vec{u}\vec{u}) = \vec{\nabla}p + \vec{\nabla}\cdot(\mu\vec{\nabla}\vec{u}) \qquad (2)$$

$$\vec{\nabla}\cdot(\rho c_p\vec{u}T) = \vec{\nabla}\cdot(k\vec{\nabla}T) \qquad (3)$$

where $\vec{u}$ is velocity vector and T and p are temperature and pressure. Also, ρ, μ, c_p and k are density, kinetic viscosity, specific heat and thermal conductivity of cooling fluid, respectively. For solid regions, equation (3) may be revised by setting: $\vec{u} = 0$ (changes the equation to pure conduction one). The operating temperature of 60°C is selected for the stack.

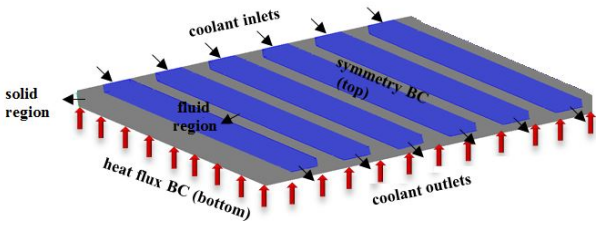

Fig. 2. Geometrical model of cooling plate (half domain) and applied boundary conditions

2.3 Boundary Conditions

The complete set of governing equations representing the mathematical model is given by Eqs. 1-3, which forms a set of equations with five unknowns: u' components, p and T. The boundary conditions are specified as follows.

i) Bottom of the cooling plate

Heat generation in the PEM fuel cell at any working voltage calculates via the V-I curve of the cell. The nominal voltage per each cell is supposed to be V_i= 0.6V. The generated heat flux per cell in the stack at any working voltage can be obtained as:

$$Q_i = (1.23 - V_i)i \qquad (4)$$

where, i is the stack output electrical current and 1.23 corresponds to the maximum voltage of a fuel cell [4]. The heat generated by fuel cell reactions is simulated as a heat flux applied on the cooling plate surface (bottom boundary in the figure 2). The heat flux is obtained via dividing the generated heat by the active area of the fuel cell. The geometric model is composed of solid region and fluid region (coolant). For present system (5kW PEM fuel cell), the average of electrical current density and the average heat flux are 6755Am^{-2} and 4255Wm^{-2}, respectively.

ii) Top of the cooling plate

Due to the symmetry condition, only half of the cooling plate is considered as the computational domain to reduce the computational costs. Symmetry condition is applied on the top boundary (the center-plane of the cooling plate), while constant heat flux condition is imposed on the bottom boundary wall sides.

There is the possibility of free-convection heat transfer with the ambient through the edges of the cooling plate. Two edges are in vertical direction and two others are in horizontal direction. The free-convective heat transfer coefficient is calculated in term of average Nusselt number. The following relations are used to obtain the average Nusselt number [21]:

$$\overline{Nu_L} = 0.27 Ra_L^{\frac{1}{4}} \qquad \text{top horizontal edge} \qquad (5)$$

$$\overline{Nu_L} = 0.15 Ra_L^{\frac{1}{3}} \qquad \text{bottom horizontal edge} \qquad (6)$$

$$\overline{Nu_L} = 0.68 + \frac{0.67 Ra_L^{\frac{1}{4}}}{(1 + (0.492/Pr)^{\frac{9}{16}})^{\frac{4}{9}}} \qquad \text{vertical edges} \qquad (7)$$

Here, L denotes the edge length, Pr is the air Prandtl number and Ra_L is Rayleigh number, represented by:

$$Ra_L = \frac{g\beta(T_s - T_\infty)L^3}{\nu\alpha} \qquad (8)$$

in which, β, ν and α are coefficient of volume expansion, kinematic viscosity and thermal diffusivity of the air, and T_s, T_∞ are the cooling plate edge and ambient temperatures, respectively. The coolant inflow temperature is supposed to be 40°C and therefore, the approximate temperature of the cooling plates at their edges is the same. All the flow properties are estimated at the film temperature [21]. The result is that the convective heat transfer coefficient at the vertical edges and top and bottom horizontal edges corresponds to 5.532, 2.84 and 6.090 Wm^{-1}K^{-1}, respectively.

iii) Inlet and outlet of channels

It is assumed that the coolant enters the flow field at a constant temperature (60°C). Inlet and outlet boundaries of fluid region are set to mass flow inlet (4 × 10^{-6} m^{3}s^{-1}) and pressure outlet conditions, respectively.

The cooling plates are made of graphite (ρ = 2250 kgm^{-3} and k= 24 Wm^{-1}K^{-1}) and the working fluid is liquid water (ρ= 983.284 kgm^{-3} and k = 0.653 Wm^{-1}K^{-1}).

2.4 NUMERICAL PROCEDURE

The discretization of the governing partial differential equations is performed by finite volume method applied to a staggered grid arrangement within the computational domain, in which different grid networks is utilized for scalar and vector variables. The

governing equations are solved by the SIMPLE algorithm assists with linking the pressure and velocity fields. The convective terms are estimated by selecting a second-order upwind scheme resulting in greater solution stability. The convergence is based on the averaged absolute value of the residual for each conservation equation and is assumed to be less than 10^{-6}, whereas the maximum relative mass residual based on the inlet mass should be smaller than 10^{-4}.

The grid dependency of numerical solution is examined for different coolant flow field designs. The tests inspect the dependency of calculated pressure drop and maximum surface temperature on the number of discretized volume cells. These two quantities become less dependent on the grid size in model A, when the cell number exceeds some 1,200,000. In model B, however, this value exceeds 1,400,000 since the bend regions with complex flow structures need higher grid density in this model.

3 RESULTS AND DISCUSSION

Initially, validation of numerical results is performed by computation of Darcy friction factor, *f*, through the pressure drop and mean velocity for a straight flow field (model A) and comparison of them with corresponding analytical data. For calculation of *f*, hydraulic diameter, D_h, is set to 1.33mm. Figure 3 depicts *f.Re* parameter along the straight channel. Also, that know the hydraulic entrance length, $L_e = 0.05 D_h \mathrm{Re}$ and applying this relation, the hydraulic entrance length for *Re*= 330 yields about 0.0219m (Compared with 0.02 obtained from numerical results as shown in figure 3). It can be seen in the figure that after this length, the simulated value of *f.Re* is converged to 61, which is relatively in good agreement with the reference value of 62 for a fully-developed laminar flow through a rectangular channel with an aspect ratio of 2 [21].

In addition of Darcy friction, here validation of numerical results is performed by computation of Nusselt number, *Nu*, for a straight flow field (model A) and comparison of them with corresponding analytical data. Available analytical solutions for thermal analysis of channel flows are usually presented under constant heat flux condition in the literatures. Here, Nusselt number is plotted along a straight channel (model A) under constant wall heat flux in figure 3. Also, the thermal entrance length is obtained from $L_{e,t} = 0.05 D_h \mathrm{Re}\,\mathrm{Pr}$. The formula results in a thermal entrance length of about 0.094m for a flow with *Re* = 330 (compared with 0.08 obtained from our numerical results, as shown in figure 3). The simulated *Nu* number converges to 3.8 after the thermal entrance length. It is also in good agreement with the reference *Nu* number of 4.12 for thermally-developed laminar flow in a rectangular channel (with aspect ratio of 2) under constant wall heat flux [22]. The little discrepancy from the reference value is due to the deviation of thermal boundary condition on the surface from constant heat flux condition.

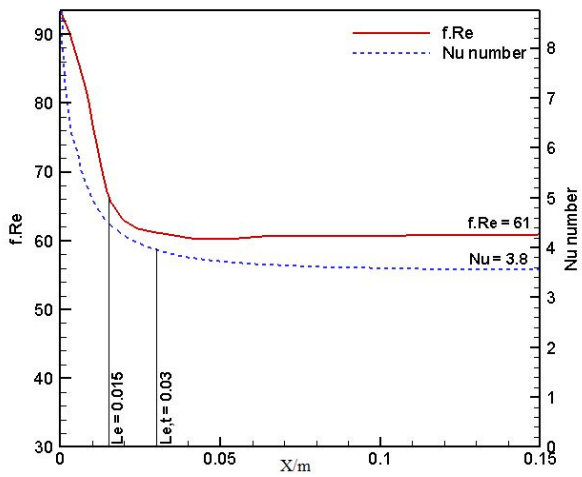

Fig. 3. Darcy friction factor and Nusselt number along a straight channel (model A).

Figure 4 displays the computed temperature distribution at the center-plane (symmetry boundary) for both models. The water temperature increases along the flow channel by absorbing the reaction heat, that is, its temperature is lowest at the inlet and highest at the outlet of the coolant flow field. The figure also represents the local water-plate temperature difference in the cooling plates for two different flow field designs, whereas the symmetry surface consists of both coolant fluid and solid regions. The cooling plates prevent overheating by properly exhausting

the reaction heat from PEM fuel cells; meantime establish a uniform temperature distribution throughout the active area.

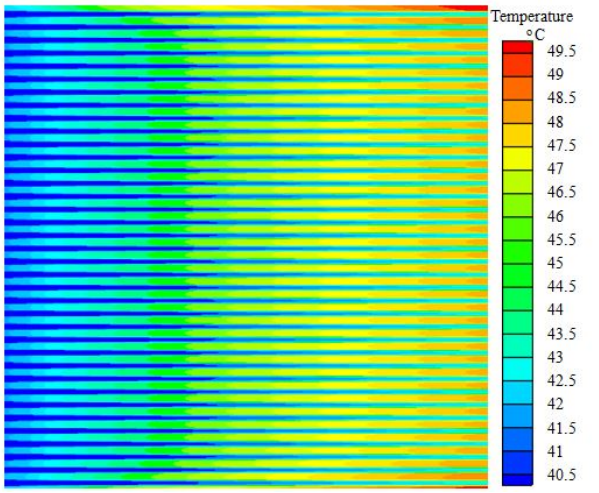

Model A

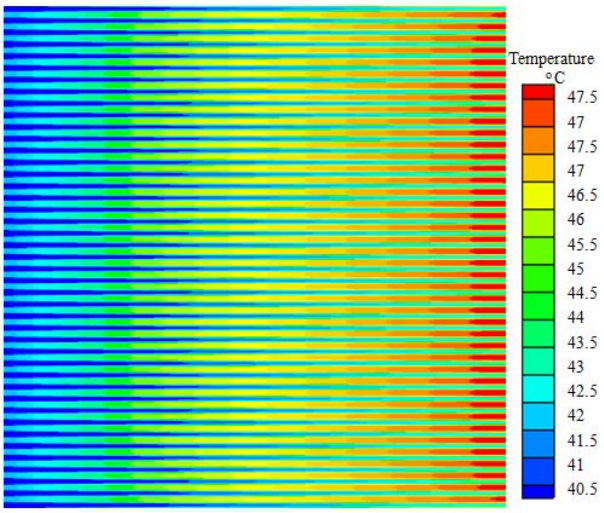

Model B

Fig. 4. Temperature distribution at the cooling plate center-plane (symmetry boundary) of models A and B

Temperature distribution at the heat transfer surface of cooling plate is shown in figure 5 for both models. It can be observed that the global temperature gradient begins from a lower temperature at the inlet and goes toward a higher value at the outlet. To make more quantitative comparison between the cooling performances, temperature uniformity index, U_T, is defined [10]:

$$U_T = \frac{\int_A |T - T_{avg}| dA}{\int_A dA}, \quad T_{avg} = \frac{\int_A T dA}{\int_A dA} \qquad (9)$$

Here, A is the surface area and T and T_{avg} are the surface and average surface temperatures, respectively. The integration in this equation is calculated only on the heat flux boundary. The temperature uniformity index can quantitatively measure the deviation of the surface temperature from the average value at the heat transfer surface. In other words, U_T becomes zero when the temperature distribution is perfectly uniform. Table 1 summarized the numerical results of two models. U_T differs between A and B models: in model A U_T is 1.85, while it is 1.7 in model B, indicating superior cooling performance of the latter model.

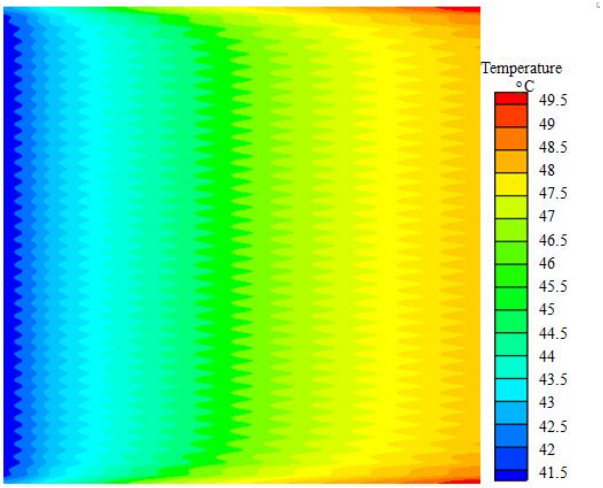

Model A

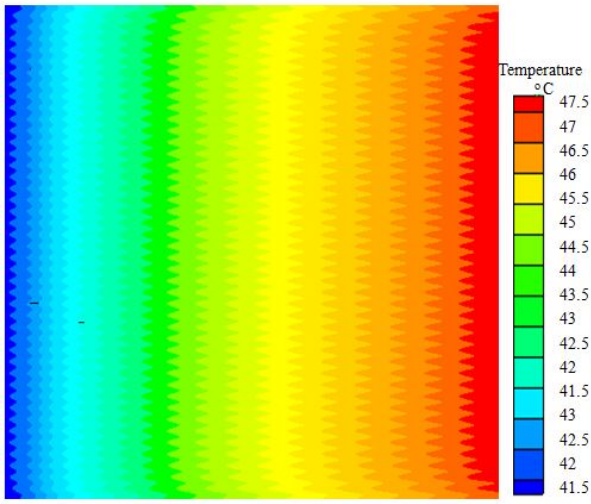

Model B

Model B

Fig.5. Temperature distribution on the heat transfer surface of cooling plate of models A and B

Table 1: Numerical outputs of two models (in °C)

Model	$T_{max,s}$	$T_{min,s}$	ΔTs	$T_{avg,s}$	U_T
A	49.9	41.1	8.7	45.4	1.85
B	47.9	41.0	6.8	45.2	1.7

To ensure the thermal stability of the cell, it is essential to control the maximum surface temperature of the cooling plate at a certain level. Indeed, it is the most important factor to prevent the thermal damaging of the cell. According to table 1 and figure 5, the maximum surface temperature of the cooling plate, $T_{max,s}$, in model B is some 2 ºC less than that of model A. On the other hand, the surface temperature difference, $\Delta T_s = T_{max,s} - T_{min,s}$ the average surface temperature, $T_{avg,s}$ and the maximum surface temperature, $T_{max,s}$, in model B are lower than the corresponding values in model A.

Figure 6 shows the coolant pressure drop (in *Pa*) along the channels for both cooling flow fields (models A and B). We see that the geometrical shape of the channel changes the coolant flow pressure drop in the cell, as influences on the maximum and average temperatures. The figure indicates that the pressure drop along rectangular and trapezoidal cross-section channels is 292.2 *Pa* and 296.4 *Pa*, respectively. This means that the pressure drop does not change significantly between two models. Nevertheless, for present models, the pressure losses are still relatively small in comparison with the serpentine channel configuration.

4 CONCLUSIONS

Fluid flow and heat transfer in cooling plates with 15 cm×15 cm square area for a water cooled polymer electrolyte membrane fuel cell was studied numerically in details. The performance of a novel cooling flow field with trapezoidal channels was precisely assessed and compared with straight channels, in terms of maximum surface temperature, temperature uniformity and pressure drop. The obtained results indicated that the maximum surface temperature, the surface temperature difference, the average surface temperature and the temperature uniformity index in a flow field with trapezoid channels all are lower than in a same model with rectangular cross-sections channels. Hence, the model with trapezoidal cross-section channels has better cooling performance. Moreover, there is a small difference between the pressure losses of two studied models. This means that cooling flow fields with trapezoidal channels is preferred to rectangular ones in terms of thermal and hydraulic characteristics. Finally, it can be concluded that parallel straight channels with trapezoidal cross-section has the potential to be used for cooling purpose in polymer electrolyte membrane fuel cells, though their manufacturing process is more expensive than rectangular geometries.

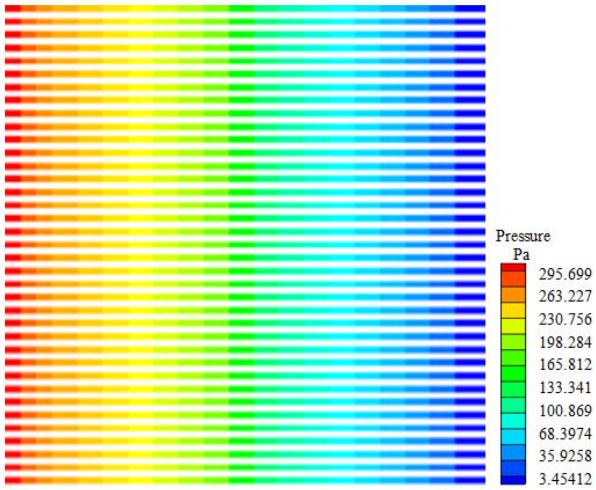

Model A

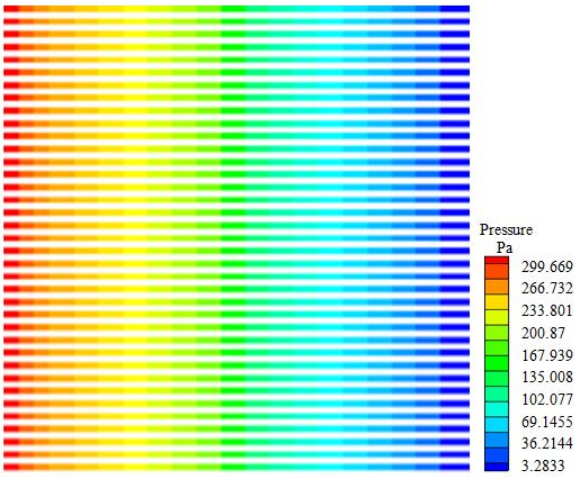

Model B

Fig. 6. Pressure distributions in cooling channels of both models

References

[1] E. Afshari, S. A. Jazayeri, Y. Mollayi Barzi, *Heat Mass Transfer* Vol. 46, 2010, pp. 1295-1305.

[2] E. Afshari, S. A. Jazayeri, *Energy Conversion and Management*, Vol. 51, 2101, pp. 655-662.

[3] S. M. H. Hashmi, PhD thesis, *Helmut Schmidt University, Hamburg, Germany*, 2010.
[4] S. Asghari, H. Akhgar, B. F. Imani, *J. Power Source*, Vol. 196**,** 2011, 3141-3148.
[5] F. C. Chen, Z. Gao, R. O. Loutfy, M. Hecht, *Fuel Cells*, Vol. 3, 2003, 181-188.
[6] K. P. Adzakpa, J. Ramousse, Y. Dubé, H. Akremi, K. Agbossou, M. Dostie A. Poulin, M. Fournier, *J. Power Sources*, Vol. 179, 2008, 16-176.
[7] S. Ravishankar, K. A. Prakash, *Applied Thermal Engineering*, Vol. 66, No. 1-2, 2014, pp. 239-251.
[8] B. D. Gould, R. Ramamurti, C. R. Osland, K. E. Swider-Lyons, *Int. J. Hydrogen Energ*, Vol. 39, 2014, pp. 14061-14070.
[9] S. Shimei, L, Wei, *Thermal Energy and Power Engineering*, Vol. 3, 2014, pp. 171-179.
[10] E. Afshari, M. Ziaei-Rad, Z. Shariat, *Int. J. of Hydrogen Energy*, Vol. 41, 2016, pp. 1902-1912.
[11] S. Yu, D. Jung, *Renewable Energy*, Vol. 33, 2008. pp. 2540-2548.
[12] J. Choi, Y. H. Kim, Y. Lee, K. J. Lee, Y. Kim, *J. Mechanical Science and Technology*, Vol. 22, 2008, pp.1417-1425.
[13] A. P. Sasmito, E. Birgersson, A. S. Mujumdar, *J. Heat Transfer Engineering*, Vol. 32, 2010, pp. 151-167.
[14] Y. Lasbet, B. Auvity, C. Castelain, H. Peerhossaini, *J. Heat Transfer Engineering*, Vol. 28, 2007, pp. 795-803.
[15] N. Guo, M. C. Leu, U. O. Koylu, *Fuel Cells*,Vol. 14, No. 6, 2014, pp. 876-885.
[16] P. J. Hamilton, B. G. Pollet, *Fuel Cells*, Vol. 10, No. 4, 2010, pp. 489-509.
[17] S. O. Olanrewaju, T. B. Ochende, J. P. Meyer, *Int. J. Energy Research*, Vol. 37, No. 3, 2013, pp. 228-241.
[18] J. Wang, H. Wang, *Fuel Cells*, Vol. 12, No. 6, 2012, pp.989-1003.
[19] E. Afshari, M. Ziaei-Rad, M. Mosharaf Dehkordi, *Journal of the Energy Institute*, Vol. 90, No. 5, 2016, pp. 752-763.
[20] G. Zhang, S. Kandlikar, *Int. J. Hydrogen Energy*, Vol. 37, 2012, pp. 2412-2429.
[21] A. Bejan, *Convection Heat Transfer*, John Wiley & Sons, 2004.
[22] F.P. Incropera, D. P. DeWitt, *Fundamentals of Heat and Mass Transfer*, John Wiley & Sons, Inc, New York, 2002.